Applied Physics Letters ARTICLE pubs.aip.org/aip/apl

Degradation of electrical properties of subcells in multi-junction solar cells under neutron irradiation

Cite as: Appl. Phys. Lett. **125**, 132105 (2024); doi: 10.1063/5.0218485
Submitted: 11 May 2024 · Accepted: 13 September 2024 ·
Published Online: 24 September 2024

Svetlana A. Levina, Viktor M. Emelyanov, Mariia V. Nakhimovich, and Maxim Z. Shvarts[a]

AFFILIATIONS

Photovoltaic Converters Lab, Ioffe Institute, St. Petersburg 194021, Russia

[a]Author to whom correspondence should be addressed: shvarts@scell.ioffe.ru

ABSTRACT

This paper presents an analysis of the photovoltaic characteristics and parameters of individual subcells of space multi-junction solar cells after irradiation by high-energy particles. Dark currents, charge carrier lifetimes, and damage coefficients for wide-bandgap subcells were determined both theoretically and experimentally.

Multi-junction (MJ) solar cells (SCs), particularly state-of-the-art GaInP–GaAs–Ge triple-junction (3J) samples, are widely used in numerous space missions. Despite the relatively high manufacturing cost of 3J SCs, they exhibit high reliability and radiation resistance during extended periods in orbit. The main threat to the performance of solar panels is the impact of high-energy particles (such as electrons, protons, neutrons, and γ-radiation) in the Earth's radiation belt on the semiconductor layers. The interaction of high-energy charged particles with SC material displaces crystal lattice atoms and forms defects, resulting in a decrease in both the SC performance and solar panel lifetime. Several techniques have been proposed to improve the radiation resistance of SC, including the embedding distributed Bragg reflectors and thinning the base layer of the GaAs subcell,[1–5] optimizing the coverglass,[6,7] and using p–i–n structures and various doping methods.[8] However, none of the known solutions can completely eliminate the negative impact of cosmic radiation. Therefore, SC degradation must be given increased attention.[9] To accurately predict the operation of SCs in orbit, it is advisable to estimate the degradation rates of semiconductor materials caused by high-energy particles, as well as the lifetimes of nonequilibrium charge carriers extracted from the dark saturation current density data.

The dark and electroluminescent characteristics of space 3J SCs have been previously studied.[10–14] Papers[11,12] closely align with the scientific and practical focus of this study, examining the characteristics of individual subcells (p–n junctions) when irradiated with high-energy protons (0.05–2.5 MeV). Electroluminescent data were used to trace dark I–V curves under BOL (beginning-of-life) and EOL (end-of-life) conditions. The possibility of analyzing both the voltage degradation of each subcell and its dark I–V curves was demonstrated at different particle energies and fluences. However, this study was limited to data on dark saturation currents and the analysis was not extended to determine the minority charge carrier lifetime in the semiconductor layers of the subcells. In Ref. 12, the main photovoltaic parameters were numerically modeled based on material data for the subcells and experimental results for MJ SCs irradiated with electrons. The minority charge carrier lifetime in each subcell semiconductor layer was also numerically evaluated, along with the corresponding damage coefficients when the samples were exposed to 1 MeV electrons. These data can be used as comparative guidelines for the research conducted in this study on the damage caused by 1.25 MeV neutrons in practical space lattice-matched 3J SCs.[15–17]

The I–V curve for a subcell with a p–n junction, neglecting the series resistance, is based on an equivalent two-diode model with distributed parameters,[18,19]

$$J = J_{ph} - J_{0s}\left[\exp\left(\frac{qV}{kT}\right) - 1\right] - J_{0r}\left[\exp\left(\frac{qV}{2kT}\right) - 1\right] - \frac{V}{R_{sh}}, \quad (1)$$

where J is the current density; J_{ph} is the light-generated photocurrent density; V is the voltage; R_{sh} is the shunt resistance; J_{0s} and J_{0r} are the dark saturation current densities according to both radiative and non-radiative recombination in the quasi-neutral n-type and p-type regions, and non-radiative recombination in the space-charge region (SCR), respectively; q is the electron charge; k is the Boltzmann constant; and T is the temperature.

The greater the number of recombination centers under radiation exposure, the higher the increase in the dark saturation current densities. In cases of severe radiation damage, when the diffusion length of minority charge carriers is shorter than the thickness of the n- and p-layers, J_{0s} can be calculated using the following equation:[20]

$$J_{0s} = q\left(\frac{n_{0p}D_n}{L_n} + \frac{p_{0n}D_p}{L_p}\right) = q\left(\frac{n_{0p}L_n}{\tau_n} + \frac{p_{0n}L_p}{\tau_p}\right), \quad (2)$$

where n_{0p}, p_{0n} represent the minority charge carrier concentrations at equilibrium; D_n, D_p are the diffusion coefficients of electrons and holes; and L_n, L_p are their respective diffusion lengths.

The saturation current density according to recombination in the quasi-neutral n-type and p-type regions is proportional to

$$J_{0s} \propto \tau_{n,p}^{-1/2}. \quad (3)$$

In the case where the diffusion lengths greatly exceeds the n- and p-layers (the initial stage of radiation damage), recombination occurs throughout the thickness of the layer,

$$J_{0s} \propto \tau_{n,p}^{-1}. \quad (4)$$

A similar process occurs in the SCR. If the field inside the SCR is weak enough and the concentrations of electrons and holes can be considered constant, then the saturation current density according to recombination in the SCR can be estimated as follows:[20]

$$J_{0r} = en_i d\tau_{eff}^{-1}, \quad (5)$$

where n_i is the intrinsic concentration of charge carriers, d is the width of the recombination region, and τ_{eff} is the effective carrier lifetime in the SCR.

If an i-layer is embedded between the n- and p-regions, and the Debye length is shorter than the thickness of this layer, then the size of the recombination region is approximately equal to the thickness of the i-layer, and the effective lifetime is equal to

$$\tau_{eff} = \tau_n + \tau_p. \quad (6)$$

In this case, a p–i–n junction can be considered as two p–i and i–n junctions connected in series. This concept applies either to p–i–n structures with a thick i-layer or to relatively high voltages, where non-equilibrium charge carriers inside the undoped region help screen the junction electric field. In practice, for GaAs p–n junctions, a similar phenomenon can be observed only when voltages exceed 1 V and the i-region is more than 0.5 μm in thickness. However, in this voltage range, the saturation current usually dominates, increasing rapidly owing to the doubling of the exponent. Consequently, the saturation current density resulting from recombination in the SCR no longer affects the shape of the I–V curves or the open-circuit voltage value.

There is another scenario that can be observed when the field of the p–n junction is sufficiently high and the boundaries of the conduction and valence bands gradually change from the donor to the acceptor doping layer. In this case, the size of the recombination region is quite small, and the effective lifetime can be calculated as

$$\tau_{eff} = \sqrt{\tau_n \tau_p}. \quad (7)$$

The high-performance SCs studied in this work are based on a well-established space-grade triple-junction GaInP/Ga(In)As/Ge heterostructure, produced using metal organic vapor phase epitaxy (MOVPE) on a Ge substrate in an upright lattice-matched configuration (practical results can be found in Refs. 9, 17, and 21–23). All subcells implemented in the MJ SCs were grown as p–n junctions, not as p–i–n junctions. Therefore, Eq. (7) is applicable for the analysis and determination of the effective lifetime of the minority carriers in the SCR (see Fig. 3).

To operate in the high-current regime (electroluminescent mode of investigation), the experimental samples (referred to below as samples #1–4) were designed in a small-size form-factor with a designated illumination area[24] S_{DIA} of 1.57 cm^2. The efficiency of the SC was recorded at 28%–29% under 1 Sun (AM0) illumination.

Samples #1–3 were irradiated with E = 1.25 MeV neutrons up to varying fluences ϕ (Table I). It should be noted that while electrons or protons are generally used in practical investigations, the specific nature of the particles is not crucial for the purposes of this research. The main focus of this study is to analyze the photovoltaic characteristics and parameters of individual subcells in the 3J SC after degradation. Sample SC#4, on the other hand, was not exposed to irradiation and was kept as a reference sample. Table I shows the displacement damage dose values for each sample,

$$D_d = \phi \cdot NIEL(E), \quad (8)$$

where $NIEL$ is the nonionizing energy loss, which is equal to 4.9×10^{-4} MeV·cm^2/g.[25] $NIEL$ was calculated for GaAs material as this material degraded faster compared to others and had the greatest impact on the output parameters of the solar battery.[26–28] D_d allows for the assessment of irradiation effects independent of the particle type (electron, proton, etc.)[29] as well as the evaluation of 3J SC characteristics following an extended period in geostationary orbit.

For each 3J SC, the external quantum efficiency (EQE) spectral dependence (Fig. 1) was studied using an optical setup and the lock-in technique.[30,31] A family of I–V curves was recorded under concentrated (up to 20×) illumination produced by a flash solar simulator with AM0 spectra.[32] This allowed to form dark I–V curves without the impact of series resistance using the I_{sc}–V_{oc} method[18] (filled symbols in Fig. 2). The dark I–V curves of the individual subcells (open symbols in Fig. 2) were obtained using a method[33] based on the reciprocity relation between the EQE of the p–n junction and its spectral dependence of electroluminescence,[34]

$$\varphi^{EL}(J) = EQE(E) \cdot \varphi^{BB} \cdot \left[\exp\left(\frac{qV(J)}{kT}\right) - 1\right], \quad (9)$$

where φ^{BB} is the black body power density at a given temperature T, and E is the radiation energy.

By transforming Eq. (9) with respect to the variable V and neglecting the "−1" term in the exponent, the I–V curve of an individual subcell can be created,

TABLE I. Fluences of irradiation.

Sample	Fluences ϕ (n/cm^{-2})	Displacement damage dose D_d (MeV/g)
SC#1	1.5×10^{13}	7.4×10^{9}
SC#2	1.5×10^{14}	7.4×10^{10}
SC#3	5×10^{14}	2.5×10^{11}

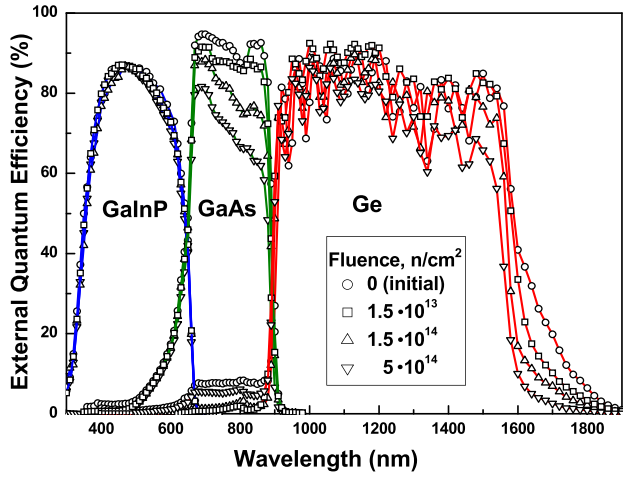

FIG. 1. EQE of samples irradiated with different fluences (see Table I).

$$V = \frac{kT}{q}\left[\ln\varphi^{EL} - \ln\mathrm{EQE} - 2\ln E + \frac{E}{kT} - \ln C\right], \tag{10}$$

where $\ln C \cdot kT/q = \delta V = const$ is introduced to account for the fact that $\varphi^{EL}(J)$ is recorded in relative units.[11] The constant δV is the same for each subcell in a given SC, independent of E and J, and is attributed only to the optical system used in the experiment. Thus, for an SC with three subcells, the total voltage $V_{MJ\,SC}$ can be found as[12]

$$V_{MJ\,SC} = \sum_i V_i - 3\delta V. \tag{11}$$

Based on the obtained dependences (see Fig. 2), the lifetimes of nonequilibrium charge carriers were determined depending on the fluence ϕ (Fig. 3). The low-doped n-layer (0.15 μm) of the GaAs subcell is almost entirely located in the SCR. The, J_{0s} current of the p–n junction is formed by carrier recombination in the p-region. The total

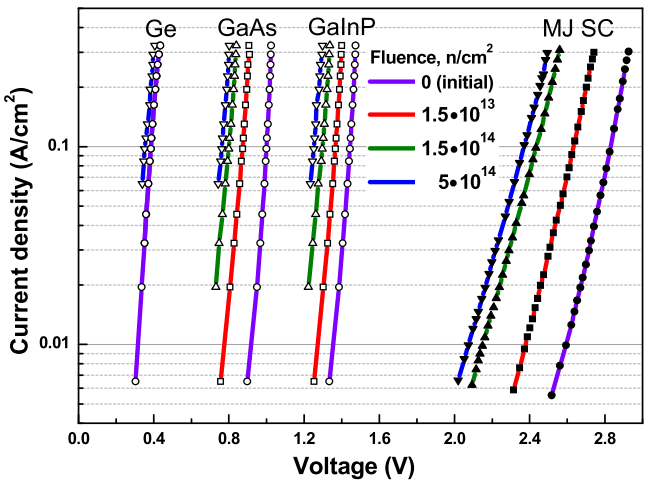

FIG. 2. Dark I–V curves of the MJ SC (filled symbols) and of individual subcells (open symbols) at different fluences of neutron irradiation (see Table I). I–V curve for the irradiated Ge subcell is presented only for the ultimate fluence of 5×10^{14} n/cm^2.

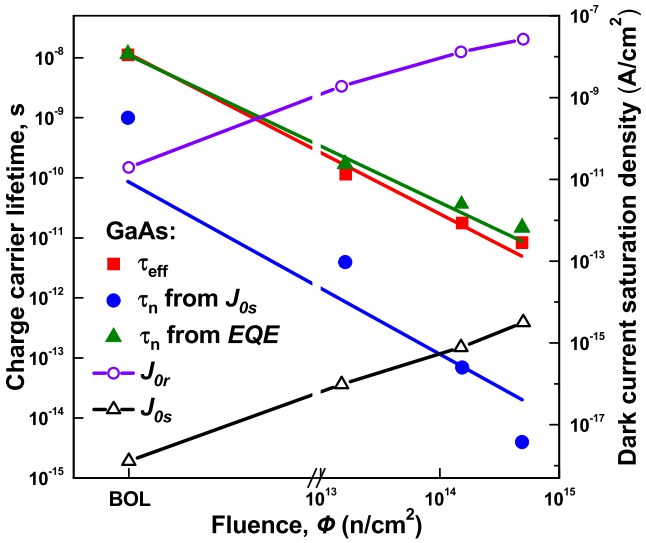

FIG. 3. Dependence of the dark saturation current densities (J_{0s}—violet open circles, J_{0r}—black open triangle) for the GaAs subcell on the fluence ϕ. Dependence of minority carrier lifetime (filled symbols): red squares represent τ_{eff}, which is the effective lifetime in the space-charge region, determined from the J_{0r} current density; blue circles represent the lifetime of electrons in the p-layer τ_n, determined from the J_{0s} current density; green triangles represent τ_n, which is determined from *EQE* (Fig. 1). The colored lines of the lifetimes show approximations of experimental dependences according to Eq. (12).

width of the SCR ranged from 0.27 to 0.29 μm depending on the subcell operating voltage. At the maximum voltage (0.988 V, corresponding to SC#4 before irradiation), the Debye length in the quasi-neutral region was 0.2 μm. Therefore, in all subcell operating modes, the built-in field of the p–n junction remained strong and uniform. The relationship between the magnitude of the J_{0r} current density and the charge carrier lifetime was established by Eq. (5). The calculation results are shown in Fig. 3 (red squares). Additionally, the lifetime of nonequilibrium electrons in the base, obtained from measured values of the diffusion current (blue circles) and *EQE* (green triangles), is provided. The minority carrier lifetime in the GaAs p-layer was determined according to Ref. 3. For each experimental *EQE* dependence, the lifetime that provided the best agreement between the calculated and experimental data was selected. The lifetime before irradiation could not be directly defined due to the small thickness of the p-layer; therefore, it was taken to be equal to 10^{-8} s, which is typical for a thicker p-GaAs layer with the same doping level grown using a similar technological process. The lines in Fig. 3 represent the approximation of the experimental dependences for lifetime τ using the following relation:[35–38]

$$\frac{1}{\tau} = \frac{1}{\tau_0} + K\Phi, \tag{12}$$

where τ_0 is the lifetime before radiation, and K is the damage coefficient of the minority carrier lifetime.

Figure 3 shows that τ_{eff} and τ_n, which reflect the effective lifetime in the SCR, which have been determined from the J_{0r}, and the lifetime in the p-layer, obtained from *EQE*, are in good agreement as well as with Eq. (12). The calculated values of the damage coefficient K for

TABLE II. Damage coefficient of minority carrier lifetime for investigated materials under irradiation, K (cm^2/s).

Material	Space-charge region	p-layer
GaInP	$(1.1 \pm 0.3) \times 10^{-5}$	...
GaAs	$(3.9 \pm 1.4) \times 10^{-4}$	$(2.2 \pm 0.8) \times 10^{-4}$

these dependences are listed in Table II. In turn, τ_n lifetimes in the p-layer, calculated using the diffusion current, are 1–2 orders of magnitude lower. The diffusion lengths of the electrons corresponding to these lifetimes are 0.2 μm and 6 nm for fluences of 1.5 $\times$ 10^{13} and 5 $\times$ 10^{14} n/cm^2, respectively, which apparently do not agree with the observed pattern of photogenerated carrier collection from the p-layer. In addition, Eq. (12) does not adequately explain the resulting dependence, making it challenging to use the J_{0s} current density for estimating radiation degradation. The underlying causes of these observed phenomena require further research. Nevertheless, this is likely due to the influence of a narrow segment of the n-layer near its boundary with a wide-bandgap window or surface recombination at this heterointerface.

The obtained dependences of the GaInP dark currents on the neutron fluences ϕ were also used to determine the lifetimes of nonequilibrium charge carriers and the damage coefficient of the material (Fig. 4 and Table II). It should be noted that the presented J_{0s} and J_{0r} values are in an agreement with the practically observed data.[39–41]

It is evident that Eq. (12) satisfactorily approximates the dependence of the effective lifetime in the GaInP SCR on the dose of damaging particles, similar to the case of GaAs. However, for the GaInP subcell, due to the minimal changes in *EQE* during irradiation, the verification of lifetime using spectral dependences was not carried out.

The effect of degradation on the main output characteristics of the 3J SC, including efficiency, fill factor, and maximum power, was determined as the ratio of the respective parameters after (EOL) and before (BOL) irradiation. The calculation results (Fig. 5) as a function of D_d for the AM0 spectrum (1 Sun) indicate that the efficiency of the 3J SC is expected to decrease by 25% after 15 years in geostationary orbit.[42]

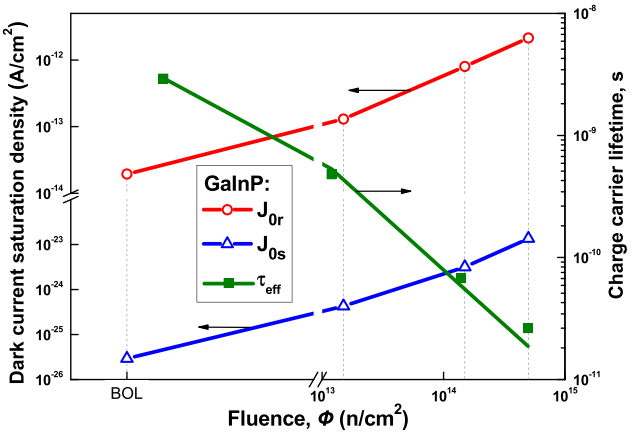

FIG. 4. Dependencies of the dark saturation current densities (red, blue open symbols) and lifetime of nonequilibrium charge carriers in the GaInP subcell (green squares) on the fluence ϕ.

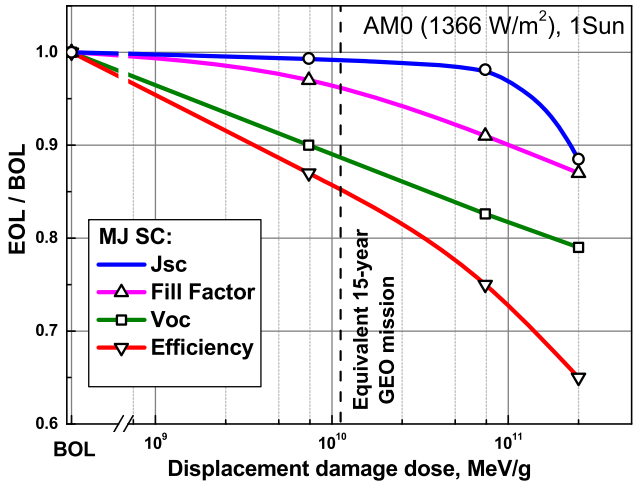

FIG. 5. Deterioration of the MJ SC output parameters (photocurrent density J_{sc}, open-circuit voltage V_{oc}, fill factor, and efficiency) depending on displacement damage dose. The red dotted line corresponds to a 15-year GEO mission.

This study focuses on the theoretical and experimental analyses of the photovoltaic characteristics of a 3J SC both before and after exposure to irradiation. Through the research, the I–V curves of individual subcells were identified at varying levels of irradiation fluences. By using these data and the two-diode equivalent model, the corresponding dark saturation currents, which are responsible for different recombination mechanisms, were determined.

The studies conducted have shown that the experimentally measured values of the J_{0r} current density can serve as an effective way to estimate the lifetime of nonequilibrium charge carriers when an SC is irradiated with high-energy particles. These values are in good agreement with the results obtained by modeling the *EQE*. However, the measured values of the J_{0s} current density at the subcell p–n junction did not provide reliable estimates of the lifetime of charge carriers in the photoactive layers or their degradation rates.

Using the developed technique, the degradation rates of the charge carrier lifetimes of the GaAs and GaInP layers were studied, and the damage factors for these materials were determined.

AUTHOR DECLARATIONS

Conflict of Interest

The authors have no conflicts to disclose.

Author Contributions

Svetlana A. Levina: Conceptualization (equal); Methodology (equal); Writing – original draft (equal); Writing – review & editing (equal). **Viktor M. Emelyanov:** Formal analysis (lead); Investigation (equal); Validation (equal). **Mariia V. Nakhimovich:** Investigation (equal). **Maxim Z. Shvarts:** Investigation (equal); Methodology (equal); Supervision (equal); Writing – original draft (equal).

DATA AVAILABILITY

The data that support the findings of this study are available from the corresponding author upon reasonable request.

REFERENCES

[1]S. J. Polly, G. T. Nelson, J. R. D'Rozario *et al.*, "Radiation effects in thinned GaAs photovoltaics incorporating DBRs for improved radiation tolerance of multijunctions," in *Proceedings of the IEEE 46th Photovoltaic Specialists Conference (PVSC)* (IEEE, 2019), pp. 2818–2821.

[2]R. Tatavarti, K. Forghani, R. Reddy *et al.*, "Radiation hardening of dual junction solar cells," in *Proceedings of the 47th IEEE Photovoltaic Specialists Conference (PVSC)* (IEEE, 2020), pp. 2258–2261.

[3]V. Emelyanov, N. Kalyuzhniy, S. Mintairov *et al.*, "Multijunction GaInP/GaInAs/Ge solar cells with Bragg reflectors," Semiconductors **44**(12), 1600–1605 (2010).

[4]M. Z. Shvarts, E. A. Aronova, V. M. Emelyanov *et al.*, "Multijunction solar cell with intermediate IR reflector," AIP Conf. Proc. **1477**(1), 28–31 (2012).

[5]V. M. Lantratov, V. M. Emelyanov, N. A. Kalyuzhnyy *et al.*, "Improvement of radiation resistance of multijunction GaInP/Ga(In)As/Ge solar cells with application of bragg reflectors," Adv. Sci. Technol. **74**, 225–230 (2010).

[6]G. P. Summers, S. R. Messenger, E. A. Burke *et al.*, "Contribution of low-energy protons to the degradation of shielded GaAs solar cells in space," Prog. Photovoltaics **5**(6), 407–413 (1997).

[7]S. R. Messenger, E. A. Burke, R. J. Walters *et al.*, "Effect of omnidirectional proton irradiation on shielded solar cells," IEEE Trans. Nucl. Sci. **53**(6), 3771–3778 (2006).

[8]T. Takamoto, H. Washio, and H. Juso, "Application of InGaP/GaAs/InGaAs triple junction solar cells to space use and concentrator photovoltaic," in *Proceedings of the IEEE 40th Photovoltaic Specialist Conference (PVSC)* (IEEE, 2014).

[9]J. M. Raya-Armenta, N. Bazmohammadi, J. C. Vasquez, and J. M. Guerrero, "A short review of radiation-induced degradation of III–V photovoltaic cells for space applications," Sol. Energy Mater. Sol. Cells **233**, 111379 (2021).

[10]G. Yan, J. Wang, J. Liu *et al.*, "Electroluminescence analysis of VOC degradation of individual subcell in GaInP/GaAs/Ge space solar cells irradiated by 1.0 MeV electrons," J. Lumin. **219**, 116905 (2020).

[11]R. Hoheisel, D. Scheiman, S. Messenger *et al.*, "Detailed characterization of the radiation response of multijunction solar cells using EL measurements," IEEE Trans. Nucl. Sci. **62**, 2894–2898 (2015).

[12]S. Roensch, R. Hoheisel, F. Dimroth *et al.*, "Subcell I-V characteristic analysis of GaInP/GaInAs/Ge solar cells using electroluminescence measurements," Appl. Phys. Lett. **98**, 251113 (2011).

[13]W. Zhang, A. Aierken, Y. Zhuang *et al.*, "Investigation of degradation characteristics of electron irradiated GaInP/InGaAs/Ge solar cell by numerical simulation model," Intl. J. Energy Res. **46**(10), 14060–14073 (2022).

[14]T. B. Wang, Z. X. Wang, S. Y. Zhang *et al.*, "1 MeV electron irradiation effect and damage mechanism analysis of flexible GaInP/GaAs/InGaAs solar cells," J. Appl. Phys. **135**(5), 053103 (2024).

[15]N. A. Pakhanov, V. M. Andreev, M. Z. Shvarts *et al.*, "State-of-the-art architectures and technologies of high-efficiency solar cells based on III–V heterostructures for space and terrestrial applications," Optoelectron. Instrum. Data Process. **54**(2), 187–202 (2018).

[16]R. Campesato, C. Baur, M. Carta *et al.*, "NIEL dose analysis on triple and single junction InGaP/GaAs/Ge solar cells irradiated with electrons, protons and neutrons," in *Proceedings of the 46th IEEE Photovoltaic Specialists Conference (PVSC 46)* (IEEE, 2019).

[17]W. Guter, F. Dunzer, L. Ebel *et al.*, "Space solar cells—3G30 and next generation radiation hard products," E3S Web Conf. **16**, 03005 (2017).

[18]M. Wolf and H. Rauschenbach, "Series resistance effects on solar cell measurements," Adv. Energy Convers. **3**(2), 455–479 (1963).

[19]P. Würfel and U. Würfel, *Physics of Solar Cells: From Basic Principles to Advanced Concepts* (John Wiley & Sons, 2016).

[20]J. L. Gray, "The physics of the solar cell," in *Handbook of Photovoltaic Science and Engineering*, 2nd ed. (John Wiley & Sons, 2011), pp. 82–129.

[21]R. Verduci, V. Romano, G. Brunetti *et al.*, "Solar energy in space applications: Review and technology perspectives," Adv. Energy Mater. **12**, 2200125 (2022).

[22]J. Li, A. Aierken, Y. Liu, Y. Zhuang *et al.*, "A brief review of high efficiency III-V solar cells for space application," Front. Phys. **8**, 631925 (2021).

[23]B. R. Uma, S. Krishnan, V. Radhakrishna, and R. Campesato, "Effect of space radiation on CTJ new version multijunction solar cells," Radiat. Eff. Defects Solids **176**(3–4), 382–395 (2021).

[24]M. A. Green, E. D. Dunlop, G. Siefer *et al.*, "Solar cell efficiency tables (Version 61)," Prog. Photovoltaics **31**(1), 3–16 (2023).

[25]M. J. Boschini, P. G. Rancoita, and M. Tacconi, see http://www.sr-niel.org/ for "SR-NIEL calculator: Screened relativistic (SR) treatment for calculating the displacement damage and nuclear stopping powers for electrons, protons, light- and heavy-ions in materials, version 4.5.1" (2019).

[26]W. Rong, L. Yunhong, and S. Xufang, "Effects of 0.28–2.80 MeV proton irradiation on GaInP/GaAs/Ge triple-junction solar cells for space use," Nucl. Instrum. Methods Phys. Res., Sect. B **266**(5), 745–749 (2008).

[27]C. Peng, F. Ding, Z. Lei *et al.*, "Investigation of radiation-induced degradations in four-junction solar cell by experiment and simulation," Microelectron. Reliab. **108**, 113646 (2020).

[28]S. Sato, T. Ohshima, and M. Imaizumi, "Modeling of degradation behavior of InGaP/GaAs/Ge triple-junction space solar cell exposed to charged particles," J. Appl. Phys. **105**, 044504 (2009).

[29]N. Gruginskie, F. Cappelluti, M. van Eerden *et al.*, "Proton irradiation induced GaAs solar cell performance degradation simulations using a physics-based model," Sol. Energy Mater. Sol. Cells **223**, 110971 (2021).

[30]M. Z. Shvarts, A. E. Chalov, E. A. Ionova *et al.*, "Indoor characterization of the multijunction III-V solar cells and concentrator modules," in Proceedings of the 20th European Photovoltaic Solar Energy Conference, Barcelona, 2005.

[31]S. A. Levina, V. M. Emelyanov, E. D. Filimonov *et al.*, "Cascade optical coupling and quantum efficiency measurements of MJ SCs," Sol. Energy Mater. Sol. Cells **213**, 110560 (2020).

[32]M. Z. Shvarts, V. R. Larionov, D. A. Malevskiy *et al.*, "Multi-lamp concepts for spectrally adjustable pulsed solar simulators," AIP Conf. Proc. **2550**, 020010 (2022).

[33]T. Kirchartz, U. Rau, M. Hermle *et al.*, "Internal voltages in GaInP/GaInAs/Ge multijunction solar cells determined by electroluminescence measurements," Appl. Phys. Lett. **92**, 123502 (2008).

[34]U. Rau, "Reciprocity relation between photovoltaic quantum efficiency and electroluminescent emission of solar cells," Phys. Rev. B **76**, 085303 (2007).

[35]J. Loferski and P. Rappaport, "Radiation damage in Ge and Si detected by carrier lifetime changes: Damage thresholds," Phys. Rev. **111**(2), 432–439 (1958).

[36]F. A. Junga and G. M. Enslow, "Radiation effects in silicon solar cells," IRE Trans. Nucl. Sci. **6**(2), 49–53 (1959).

[37]W. Rosenzweig, H. K. Gummel, and F. M. Smits, "Solar cell degradation under 1-MeV electron bombardment," Bell Syst. Tech. J. **42**(2), 399–414 (1963).

[38]W. Rosenzweig, F. M. Smits, and W. L. Brown, "Energy dependence of proton irradiation damage in silicon," J. Appl. Phys. **35**(9), 2707–2711 (1964).

[39]R. Hoheisel, F. Dimroth, A. W. Bett *et al.*, "Electroluminescence analysis of irradiated GaInP/GaInAs/Ge space solar cells," Sol. Energy Mater. Sol. Cells **108**, 235–240 (2013).

[40]J. F. Geisz, R. M. France, K. L. Schulte *et al.*, "Six-junction III–V solar cells with 47.1% conversion efficiency under 143 suns concentration," Nat. Energy **5**(4), 326–335 (2020).

[41]M. A. Mintairov, V. V. Evstropov, S. A. Mintairov *et al.*, "Current invariant as fundamental relation between saturation currents and band gaps for semiconductor solar cells," Sol. Energy Mater. Sol. Cells **264**, 112619 (2024).

[42]S. R. Messenger, G. P. Summers, E. A. Burke *et al.*, "Modeling solar cell degradation in space: A comparison of the NRL displacement damage dose and the JPL equivalent fluence approaches," Prog. Photovoltaics **9**, 103 (2001).